SFB/CPP-08-82
DESY 08-135
LTH 809
HU-EP-08/44

The static-light meson spectrum from twisted mass lattice QCD

Karl Jansen
DESY, Platanenallee 6, D-15738 Zeuthen, Germany
karl.jansen@desy.de

Chris Michael, Andrea Shindler
Theoretical Physics Division, Department of Mathematical Sciences, University of Liverpool, Liverpool L69 3BX, UK
c.michael@liverpool.ac.uk
andrea.shindler@liverpool.ac.uk

Marc Wagner
Humboldt-Universität zu Berlin, Institut für Physik, Newtonstraße 15, D-12489 Berlin, Germany
mcwagner@physik.hu-berlin.de

October 9, 2008

Abstract

We compute the static-light meson spectrum with $N_f = 2$ flavours of sea quarks using Wilson twisted mass lattice QCD. We consider five different values for the light quark mass corresponding to $300\,\mathrm{MeV} \lesssim m_{\mathrm{PS}} \lesssim 600\,\mathrm{MeV}$ and we present results for angular momentum $j = 1/2$, $j = 3/2$ and $j = 5/2$ and for parity $\mathcal{P} = +$ and $\mathcal{P} = -$. We extrapolate our results to physical quark masses and make predictions regarding the spectrum of B and B_s mesons.

1 Introduction

A systematic way to study B and B_s mesons from first principles is with lattice QCD. Since $am_b > 1$ at currently available lattice spacings for large volume simulations, one needs to use for the b quark a formalism such as Heavy Quark Effective Theory (HQET) or Non-Relativistic QCD. Here we follow the HQET route, which enables all sources of systematic error to be controlled.

In the static limit a heavy-light meson will be the "hydrogen atom" of QCD. Since in this limit there are no interactions involving the heavy quark spin, states are doubly degenerate, i.e. there is no hyperfine splitting. Therefore, it is common to label static-light mesons by parity $\mathcal{P}$ and total angular momentum of the light degrees of freedom j with $j = |l \pm 1/2|$, where l denotes angular momentum and $\pm 1/2$ the spin of the light quark. An equivalent notation is given by $S \equiv (1/2)^-$, $P_- \equiv (1/2)^+$, $P_+ \equiv (3/2)^+$, $D_- \equiv (3/2)^-$, ... The total angular momentum of the static-light meson is either $J = j + 1/2$ or $J = j - 1/2$, where both states are of the same mass. Note that in contrast to parity, charge conjugation is not a good quantum number, since static-light mesons are made from non-identical quarks.

The static-light meson spectrum has been studied comprehensively by lattice methods in the quenched approximation with a rather coarse lattice spacing [1]. Lattice studies with $N_f = 2$ flavours of dynamical sea quarks have also explored this spectrum [2, 3, 4, 5, 6, 7]. Here (cf. also [8]) we use $N_f = 2$ and are able to reach lighter dynamical quark masses, which are closer to the physical u/d quark mass, so enabling a more reliable extrapolation. Note that in this formalism, mass differences in the heavy-light spectrum are $\mathcal{O}(a)$ improved so that the continuum limit is more readily accessible.

In this paper, we concentrate on the unitary sector, where valence quarks and sea quarks are of the same mass. This is appropriate for static-light mesons with a light quark, which is u/d. We also estimate masses of static-light mesons with light s quarks, albeit with a sea of two degenerate s instead of u and d. Within the twisted mass formalism, it is feasible to use $N_f = 2 + 1 + 1$ flavours of dynamical sea quarks, which will give a more appropriate focus on the static-strange meson spectrum with light sea quarks.

In HQET the leading order is just the static limit. The next correction will be of order $1/m_Q$, where m_Q is the mass of the heavy quark. This correction is expected be relatively small for b quarks, but larger for c quarks. Lattice methods to evaluate these $1/m_Q$ contributions to the B meson hyperfine splittings have been established and tested in quenched studies [9, 10]. We intend to explore these contributions using lattice techniques subsequently. An alternative way to predict the spectrum for B and B_s mesons is to interpolate between D and D_s states, where the experimental spectrum is rather well known, and the static limit obtained by lattice QCD assuming a dependence as $1/m_Q$. Thus the splittings among B and B_s mesons should be approximately $m_c/m_b \approx 1/3$ of those among the corresponding D and D_s mesons.

For excited D_s mesons, experiment has shown that some of the states have very narrow decay widths [11]. This comes about, since the hadronic transitions to DK and D_sM (where M is a flavour singlet mesonic system, e.g. η', $\pi\pi$ or f_0) are not allowed energetically. The isospin violating decay to $D_s\pi$ together with electromagnetic decay to $D_s\gamma$ are then responsible for the narrow width observed. A similar situation may exist for B_s decays and we investigate this here using our lattice mass determinations of the excited states. This will enable us to predict

whether narrow excited B_s mesons should be found.

As well as exploring this issue of great interest to experiment, we determine the excited state spectrum of static-light mesons as fully as possible. This will help the construction of phenomenological models and will shed light on questions such as, whether there is an inversion of the level ordering with l_+ lighter than l_- at larger l or for radial excitations as has been predicted [12, 13, 14, 15].

Since we measure the spectrum for a range of values of the bare quark mass parameter $\mu_{\rm q}$ for the light quark, we could also compare with chiral effective Lagrangians appropriate to HQET. This comparison would be most appropriate applied to heavy-light decay constants in the continuum limit, so we will defer that discussion to a subsequent publication.

This paper is organised as follows. In section 2 we review some basic properties of twisted mass lattice QCD. Moreover, we discuss particularities arising in static-light computations as well as automatic $\mathcal{O}(a)$ improvement. In section 3 we present technical details regarding static-light meson creation operators and the corresponding correlation matrices we are using. We also explain how we extract the static-light spectrum from these correlation matrices and present numerical results for a range of light quark masses. We extrapolate these results both to the physical u/d quark mass and to the physical s quark mass. In section 4 we make predictions regarding the spectrum of B and B_s mesons by interpolating in the heavy quark mass to the physical b quark mass using experimental results as input. We close with a summary and a brief outlook (section 5).

2 Twisted mass lattice QCD

2.1 Simulation details

We use $L^3 \times T = 24^3 \times 48$ gauge configurations produced by the European Twisted Mass Collaboration (ETMC). The gauge action is the tree-level Symanzik (tlSym) action [16]

$$S_{\rm G}[U] \;=\; \frac{\beta}{6}\Big(b_0 \sum_{x,\mu\neq\nu} {\rm Tr}\Big(1 - P^{1\times 1}(x;\mu,\nu)\Big) + b_1 \sum_{x,\mu\neq\nu} {\rm Tr}\Big(1 - P^{1\times 2}(x;\mu,\nu)\Big)\Big) \tag{1}$$

with the normalisation condition $b_0 = 1 - 8b_1$ and $b_1 = -1/12$. The fermionic action is the Wilson twisted mass (Wtm) action [17, 18, 19] with $N_f = 2$ degenerate flavours

$$S_{\rm F}[\chi,\bar{\chi},U] \;=\; a^4 \sum_x \bar{\chi}(x)\Big(D_{\rm W} + i\mu_{\rm q}\gamma_5\tau_3\Big)\chi(x), \tag{2}$$

where

$$D_{\rm W} \;=\; \frac{1}{2}\Big(\gamma_\mu\Big(\nabla_\mu + \nabla^*_\mu\Big) - a\nabla^*_\mu\nabla_\mu\Big) + m_0, \tag{3}$$

∇_μ and ∇^*_μ are the standard gauge covariant forward and backward derivatives, m_0 and $\mu_{\rm q}$ are the bare untwisted and twisted quark masses respectively and $\chi = (\chi^{(u)}\,,\,\chi^{(d)})$ represents the fermionic field in the so-called twisted basis. It is useful to introduce at this point the twist angle

ω given by $\tan\omega = \mu_{\rm R}/m_{\rm R}$, where $\mu_{\rm R}$ and $m_{\rm R}$ denote the renormalised twisted and untwisted quark masses. This angle characterises the particular lattice action and must be kept fixed up to $\mathcal{O}(a)$, while performing the continuum limit.

The results presented in this paper have been obtained with gauge configurations computed at $\beta = 3.9$ corresponding to a lattice spacing $a = 0.0855(5)\,\mathrm{fm}$. We consider five different values of $\mu_{\rm q}$ with m_0 tuned to its critical value at $\mu_{\rm q} = 0.0040$ [20, 21, 22] (cf. Table 1, where for each value the corresponding "pion mass" $m_{\rm PS}$ and number of gauge configurations is listed). With this tuning our target continuum theory is given by

$$\mathcal{L} \;=\; \bar{\chi}(x)\Big(\gamma_\mu D_\mu + i\mu_{\rm R}\gamma_5\tau_3\Big)\chi(x), \tag{4}$$

which is parameterised by the renormalised twisted quark mass $\mu_{\rm R}$. The tuning guarantees automatic $\mathcal{O}(a)$ improvement for physical correlation functions involving only light fermions [18]. In section 2.3 we will argue that automatic $\mathcal{O}(a)$ improvement also holds for static-light spectral quantities without additional complications.

$\mu_{\rm q}$	$m_{\rm PS}$ in MeV	number of gauge configurations
0.0040	314(2)	1400
0.0064	391(1)	1450
0.0085	448(1)	1350
0.0100	485(1)	900
0.0150	597(2)	1000

Table 1: bare twisted quark masses $\mu_{\rm q}$, pion masses $m_{\rm PS}$ and number of gauge configurations.

2.2 Static-light correlation functions

To compute correctly a static-light correlation function with the Wtm lattice action (2), we follow the general procedure described in [17] and reviewed in [19]. The procedure reads:

(1) start with the continuum static-light correlation function you are interested in,

(2) perform the axial rotation

$$\psi \;=\; \exp\Big(i\omega\gamma_5\tau_3/2\Big)\chi \quad , \quad \bar{\psi} \;=\; \bar{\chi}\exp\Big(i\omega\gamma_5\tau_3/2\Big) \tag{5}$$

on the fields appearing in the correlation function with a given value for ω,

(3) compute the resulting correlation function with the Wtm lattice action (2), with a choice of quark masses, such that $\tan\omega = \mu_{\rm R}/m_{\rm R}$ up to $\mathcal{O}(a)$,

(4) perform the continuum limit with renormalisation constants computed in a massless scheme, tuning the untwisted bare quark mass in order to achieve the desired target continuum theory, i.e. the desired value of the twist angle ω.

Each value of ω defines a different discretisation, but when the continuum limit is performed the result will be exactly the initially chosen static-light correlation function in the continuum with quark mass $M_{\rm R}^2 = m_{\rm R}^2 + \mu_{\rm R}^2$.

In the following we give an explicit example. In QCD the pseudoscalar and scalar static-light currents read

$$\mathcal{P}^{\rm stat}(x) \;=\; \bar{Q}(x)\gamma_5\psi^{(u)}(x) \quad , \quad \mathcal{S}^{\rm stat}(x) \;=\; \bar{Q}(x)\psi^{(u)}(x), \tag{6}$$

where Q is the static quark field[1] and $\psi^{(u)}$ is a single flavour of the light fermion doublet $\psi = (\psi^{(u)}\,,\,\psi^{(d)})$. Let us suppose we are interested in computing in continuum QCD the static-light pseudoscalar-pseudoscalar correlation function

$$\mathcal{C}_{\mathcal{PP}} \;=\; \Big\langle (\mathcal{P}^{\rm stat})_{\rm R}(x)(\mathcal{P}^{\rm stat})^\dagger_{\rm R}(y)\Big\rangle_{(M_{\rm R},0)}, \tag{7}$$

where we write an index $(M_{\rm R},0)$ to specify that the continuum action has a vanishing twisted mass and a renormalised untwisted mass given by $M_{\rm R}$. We perform the axial rotation (5) obtaining

$$\cos^2(\omega/2)Z_{\rm P}^2 C_{\rm PP} + \sin^2(\omega/2)Z_{\rm S}^2 C_{\rm SS} - i\cos(\omega/2)\sin(\omega/2)Z_{\rm P}Z_{\rm S}\Big(C_{\rm PS} - C_{\rm SP}\Big), \tag{8}$$

where $Z_{\rm P}$ and $Z_{\rm S}$ are the standard renormalisation constants for static-light currents computed in a massless scheme with Wilson fermions. Note that for the static-light case, $Z_{\rm V} \equiv Z_{\rm P}$ and $Z_{\rm A} \equiv Z_{\rm S}$. This correlation function has to be computed with the Wtm action (2) with quark masses tuned accordingly to the value of ω chosen. The $C_{\rm XX}$ correlation functions in (8) are defined in terms of currents in the twisted basis

$$C_{\rm PP} \;=\; \Big\langle P^{\rm stat}(x)(P^{\rm stat})^\dagger(y)\Big\rangle_{(m_{\rm R},\mu_{\rm R})} \quad , \quad C_{\rm SS} \;=\; \Big\langle S^{\rm stat}(x)(S^{\rm stat})^\dagger(y)\Big\rangle_{(m_{\rm R},\mu_{\rm R})} \quad , \quad \ldots, \tag{9}$$

where

$$P^{\rm stat}(x) \;=\; \bar{Q}\gamma_5\chi^{(u)}(x) \quad , \quad S^{\rm stat}(x) \;=\; \bar{Q}(x)\chi^{(u)}(x). \tag{10}$$

Once the continuum limit of the correlation function (8) has been performed, the result will be the original correlation function (7) with $M_{\rm R}^2 = m_{\rm R}^2 + \mu_{\rm R}^2$.

However, to compute spectral quantities it is sufficient to analyze a matrix of correlation functions of bare currents with the appropriate quantum numbers. We will discuss this in detail in section 2.4.

2.3 Automatic $\mathcal{O}(a)$ improvement of static-light meson masses

Spectral quantities like hadron masses extracted from lattice simulations of Wilson fermions will in general be affected by $\mathcal{O}(a)$ discretisation errors. In the particular case of masses extracted

[1] We will discuss the static quark action in section 3.2.1.

from static-light correlation functions the $\mathcal{O}(a)$ discretisation errors come from the dimension-5-operators of the Symanzik effective action of the light and static quarks.

The Symanzik effective action for the Eichten-Hill (EH) static action contains only one term, which contributes to the $\mathcal{O}(a)$ corrections of the linearly divergent static self-energy [23]. In this paper all observables we consider are differences, where this static self-energy cancels. Moreover, this result is independent on the particular lattice static action chosen, as long as it preserves the relevant symmetries of the EH action. This is the case for our choice of static action (cf. section 3.2.1).

As a consequence, the only $\mathcal{O}(a)$ errors which could affect our results, come from the dimension-5-operators of the Symanzik effective action of the light quarks. The light quark action used in this paper is Wtm at maximal twist. It is by now well known that at maximal twist a single insertion of a dimension-5-operator of the Symanzik effective action into parity even correlation functions vanishes, because, independently on the lattice basis adopted, these operators are parity odd and the insertions have to be evaluated in the continuum theory, where parity is a preserved symmetry [18]. We can conclude that all the spectral quantities, when the static self-energy has been removed, are automatically $\mathcal{O}(a)$ improved.

2.4 Spectral decomposition and parity mixing

In this section we explain, how to analyze lattice results for static-light correlation functions obtained in the twisted basis. In particular we concentrate on the assignment of parity labels to extracted static-light meson states.

We start from the physical basis and, for simplicity, consider only two operators, the pseudoscalar and the scalar static-light current, and only two states, which we label by $|1\rangle$ and $|2\rangle$. The explanation carries over to the more general case in a straightforward way.

First consider the following matrix of correlation functions in the physical basis:

$$\mathcal{C}(t) \;=\; \begin{pmatrix} \mathcal{C}_{\mathcal{PP}}(t) & \mathcal{C}_{\mathcal{PS}}(t) \\ \mathcal{C}_{\mathcal{SP}}(t) & \mathcal{C}_{\mathcal{SS}}(t) \end{pmatrix}, \tag{11}$$

where $\mathcal{C}_{\mathcal{PP}}(t)$ has been defined in (7) with $x = (t, \vec{0})$ and $y = (0, \vec{0})$ and analogously the others. The parity of the operators $(\mathcal{P}^{\mathrm{stat}})_{\mathrm{R}}$ and $(\mathcal{S}^{\mathrm{stat}})_{\mathrm{R}}$ is determined by the parity transformation properties of the associated field, i.e. $(\mathcal{P}^{\mathrm{stat}})_{\mathrm{R}}$ has negative parity and $(\mathcal{S}^{\mathrm{stat}})_{\mathrm{R}}$ has positive parity. Even if parity is broken at finite lattice spacing, one can still assign a parity label to each of the states we use to decompose the correlation functions [18]. If we consider only two states, the spectral decomposition will have the form

$$\mathcal{C}(T) \;=\; \begin{pmatrix} |a_1^{\mathcal{P}}|^2 & (a_1^{\mathcal{P}})^* a_1^{\mathcal{S}} \\ (a_1^{\mathcal{S}})^* a_1^{\mathcal{P}} & |a_1^{\mathcal{S}}|^2 \end{pmatrix} e^{-M_1 t} + \begin{pmatrix} |a_2^{\mathcal{P}}|^2 & (a_2^{\mathcal{P}})^* a_2^{\mathcal{S}} \\ (a_2^{\mathcal{S}})^* a_2^{\mathcal{P}} & |a_2^{\mathcal{S}}|^2 \end{pmatrix} e^{-M_2 t}, \tag{12}$$

where we have defined

$$(a_{1,2}^{\mathcal{P}})^* \;=\; \langle \Omega | \hat{\mathcal{P}}^{\mathrm{stat}} | 1,2 \rangle \quad , \quad (a_{1,2}^{\mathcal{S}})^* \;=\; \langle \Omega | \hat{\mathcal{S}}^{\mathrm{stat}} | 1,2 \rangle. \tag{13}$$

The correlation functions $\mathcal{C}_{\mathcal{PS}}$ and $\mathcal{C}_{\mathcal{SP}}$ vanish in the continuum limit, because parity is a symmetry of QCD. This means by universality that at finite lattice spacing they are at most of

$\mathcal{O}(a)$. Since $\mathcal{C}_{\mathcal{PP}}$ and $\mathcal{C}_{\mathcal{SS}}$ are of $\mathcal{O}(1)$ in the continuum limit, we can conclude that for given n either $a_n^{\mathcal{P}}$ is of $\mathcal{O}(1)$ and $a_n^{\mathcal{S}}$ is of $\mathcal{O}(a)$ or the opposite way round [18]. We can conclude that if $a_n^{\mathcal{P}}$ is of $\mathcal{O}(1)$, the state $|n\rangle$ has the same parity as the formal parity of $\mathcal{P}^{\mathrm{stat}}$, which in this case is negative. Moreover, $a_n^{\mathcal{S}}$ is of $\mathcal{O}(a)$ and has to vanish in the continuum limit.

We now perform the axial transformation (5). The relation between correlation functions up to discretisation errors is, for example, for $\mathcal{C}_{\mathcal{PP}}$

$$\mathcal{C}_{\mathcal{PP}} = \cos^2(\omega/2) Z_{\mathrm{P}}^2 C_{\mathrm{PP}} + \sin^2(\omega/2) Z_{\mathrm{S}}^2 C_{\mathrm{SS}} - i \cos(\omega/2)\sin(\omega/2) Z_{\mathrm{P}} Z_{\mathrm{S}} \Big(C_{\mathrm{PS}} - C_{\mathrm{SP}} \Big). \tag{14}$$

For the matrix of correlation functions in the twisted basis

$$C(t) = \begin{pmatrix} C_{\mathrm{PP}}(t) & C_{\mathrm{PS}}(t) \\ C_{\mathrm{SP}}(t) & C_{\mathrm{SS}}(t) \end{pmatrix} \tag{15}$$

we can also perform a spectral decomposition considering again only the states $|1\rangle$ and $|2\rangle$:

$$C(t) = \begin{pmatrix} |b_1^{\mathrm{P}}|^2 & (b_1^{\mathrm{P}})^* b_1^{\mathrm{S}} \\ (b_1^{\mathrm{S}})^* b_1^{\mathrm{P}} & |b_1^{\mathrm{S}}|^2 \end{pmatrix} e^{-M_1 t} + \begin{pmatrix} |b_2^{\mathrm{P}}|^2 & (b_2^{\mathrm{P}})^* b_2^{\mathrm{S}} \\ (b_2^{\mathrm{S}})^* b_2^{\mathrm{P}} & |b_2^{\mathrm{S}}|^2 \end{pmatrix} e^{-M_2 t}. \tag{16}$$

From (12), (14) and (16) we can conclude

$$|a_{1,2}^{\mathcal{P}}|^2 = \cos^2(\omega/2) Z_{\mathrm{P}}^2 |b_{1,2}^{\mathrm{P}}|^2 + \sin^2(\omega/2) Z_{\mathrm{S}}^2 |b_{1,2}^{\mathrm{S}}|^2 + 2\cos(\omega/2)\sin(\omega/2) Z_{\mathrm{P}} Z_{\mathrm{S}} \mathrm{Im}\Big((b_{1,2}^{\mathrm{P}})^* b_{1,2}^{\mathrm{S}} \Big) \tag{17}$$

$$|a_{1,2}^{\mathcal{S}}|^2 = \cos^2(\omega/2) Z_{\mathrm{S}}^2 |b_{1,2}^{\mathrm{S}}|^2 + \sin^2(\omega/2) Z_{\mathrm{P}}^2 |b_{1,2}^{\mathrm{P}}|^2 + 2\cos(\omega/2)\sin(\omega/2) Z_{\mathrm{P}} Z_{\mathrm{S}} \mathrm{Im}\Big((b_{1,2}^{\mathrm{S}})^* b_{1,2}^{\mathrm{P}} \Big). \tag{18}$$

If the state $|1\rangle$ has negative parity, $|a_1^{\mathcal{S}}|^2$ has to vanish as $\mathcal{O}(a^2)$ in the continuum limit, while $|a_1^{\mathcal{P}}|^2$ has to be of $\mathcal{O}(1)$. Since the first two terms on the right hand side of (17) are positive and non-vanishing in the continuum limit, there must be a cancellation coming from the third term. In fact we immediately see that this third term has opposite sign for $|a_{1,2}^{\mathcal{P}}|^2$ compared to $|a_{1,2}^{\mathcal{S}}|^2$. This allows us to identify the parity of the states $|1\rangle$ and $|2\rangle$ without knowing the exact values of the renormalisation constants and the twist angle. The criterion will be the following: if

$$\mathrm{Im}\Big((b_1^{\mathrm{S}})^* b_1^{\mathrm{P}} \Big) < 0, \tag{19}$$

the state $|1\rangle$ has negative parity, otherwise positive parity. The other cases follow accordingly.

This method, which we have described for a simple case, is valid independently of the number of states considered and the kind of operators studied. At finite lattice spacing it provides a way to assign a formal parity to each of the extracted states.

The method extends to all cases, where the light degrees of freedom involve fermions in the twisted basis, e.g. for static-light mesons, but also for baryons.

3 The static-light meson spectrum

3.1 Static-light trial states

3.1.1 Static-light meson creation operators in the continuum

It is convenient to discuss static-light mesons treating the static quark as a four component spinor since the symmetries of hadronic bilinears are well studied [24]. In the continuum an operator creating a static-light meson with well defined quantum numbers J , j and $\mathcal{P}$ is given by

$$\mathcal{O}^{(\Gamma)}(\mathbf{x}) \;=\; \bar{Q}(\mathbf{x}) \int d\hat{\mathbf{n}}\, \Gamma(\hat{\mathbf{n}}) U(\mathbf{x}; \mathbf{x}+r\hat{\mathbf{n}}) \psi^{(u)}(\mathbf{x}+r\hat{\mathbf{n}}). \tag{20}$$

$\bar{Q}(\mathbf{x})$ represents an infinitely heavy antiquark (here a Dirac spinor) at position $\mathbf{x}$, $\int d\hat{\mathbf{n}}$ denotes an integration over the unit sphere, U is a straight parallel transporter and $\psi^{(u)}(\mathbf{x}+r\hat{\mathbf{n}})$ creates a light quark at position $\mathbf{x}+r\hat{\mathbf{n}}$ separated by a distance r from the antiquark (of course, using $\psi^{(d)}$ instead of $\psi^{(u)}$ would yield identical results). Γ is an appropriate combination of spherical harmonics and γ matrices coupling angular momentum and quark spin to yield well defined total angular momentum J (static quark spin included) and j (static quark spin not included) and parity $\mathcal{P}$. The meson creation operators used in the following are listed in Table 2.

$\Gamma(\hat{\mathbf{n}})$	$J^{\mathcal{P}}$	$j^{\mathcal{P}}$	$\mathrm{O_h}$	lattice $j^{\mathcal{P}}$	notation
γ_5 , $\gamma_5\gamma_j\hat{n}_j$	0^- $[1^-]$	$(1/2)^-$	A_1	$(1/2)^-$, $(7/2)^-$, ...	S
1 , $\gamma_j\hat{n}_j$	0^+ $[1^+]$	$(1/2)^+$		$(1/2)^+$, $(7/2)^+$, ...	P_-
$\gamma_1\hat{n}_1-\gamma_2\hat{n}_2$ (and cyclic)	2^+ $[1^+]$	$(3/2)^+$	E	$(3/2)^+$, $(5/2)^+$, ...	P_+
$\gamma_5(\gamma_1\hat{n}_1-\gamma_2\hat{n}_2)$ (and cyclic)	2^- $[1^-]$	$(3/2)^-$		$(3/2)^-$, $(5/2)^-$, ...	$D_\pm$
$\gamma_1\hat{n}_2\hat{n}_3+\gamma_2\hat{n}_3\hat{n}_1+\gamma_3\hat{n}_1\hat{n}_2$	3^- $[2^-]$	$(5/2)^-$	A_2	$(5/2)^-$, $(7/2)^-$, ...	D_+
$\gamma_5(\gamma_1\hat{n}_2\hat{n}_3+\gamma_2\hat{n}_3\hat{n}_1+\gamma_3\hat{n}_1\hat{n}_2)$	3^+ $[2^+]$	$(5/2)^+$		$(5/2)^+$, $(7/2)^+$, ...	$F_\pm$

Table 2: Static-light meson creation operators. The other mesonic $J^{\mathcal{P}}$ states that are degenerate with that created are noted in square brackets.

3.1.2 Static-light meson creation operators on a lattice

Here we present the construction of appropriate lattice operators to create the states of interest, following [1, 24]. When putting static-light meson creation operators (20) on a lattice, one has to replace the integration over the unit sphere by a discrete sum over lattice sites, which have the same distance from the static antiquark at position $\mathbf{x}$. For the operators in A_1 and E representations we use six lattice sites, i.e.

$$\mathcal{O}^{(\Gamma)}(\mathbf{x}) \;=\; \bar{Q}(\mathbf{x}) \sum_{\mathbf{n}=\pm\hat{\mathbf{e}}_1,\pm\hat{\mathbf{e}}_2,\pm\hat{\mathbf{e}}_3} \Gamma(\hat{\mathbf{n}}) U(\mathbf{x}; \mathbf{x}+r\mathbf{n}) \chi^{(u)}(\mathbf{x}+r\mathbf{n}), \tag{21}$$

whereas for those in the A_2 representation one has to use eight lattice sites, i.e.

$$\mathcal{O}^{(\Gamma)}(\mathbf{x}) \quad = \quad \bar{Q}(\mathbf{x}) \sum_{\mathbf{n}=\pm\hat{\mathbf{e}}_1\pm\hat{\mathbf{e}}_2\pm\hat{\mathbf{e}}_3} \Gamma(\hat{\mathbf{n}}) U(\mathbf{x};\mathbf{x}+r\mathbf{n}) \chi^{(u)}(\mathbf{x}+r\mathbf{n}). \tag{22}$$

In the first case the spatial parallel transporters are straight paths of links, while in the second case we use "diagonal links", which are averages over the six possible paths around a cube between opposite corners projected back to SU(3).

The states created by these lattice meson creation operators do not form irreducible representations of the rotation group SO(3), but of its cubic subgroup $\mathrm{O_h}$. Therefore, these states have no well defined total angular momentum, but are linear superpositions of an infinite number of total angular momentum eigenstates. The common notation of the corresponding $\mathrm{O_h}$ representations together with their lowest angular momentum content are also listed in Table 2. Note that we do not consider $\mathrm{O_h}$ representations T_1 and T_2, because these representations yield correlation functions, which are numerically identical to those listed (e.g. T_1 would be $\Gamma = \gamma_j$ or $\Gamma = \gamma_5\gamma_j$, which gives the same correlations as $\Gamma = \gamma_5$ and $\Gamma = 1$, and T_2 would be $\Gamma = \gamma_1 n_2 + \gamma_2 n_1$ or $\Gamma = \gamma_5(\gamma_1 n_2 + \gamma_2 n_1)$, which gives the same correlations as $\Gamma = \gamma_1 n_1 - \gamma_2 n_2$ and $\Gamma = \gamma_5(\gamma_1 n_1 - \gamma_2 n_2)$).

Since the D_- and the D_+ states as well as the F_- and F_+ states are expected to have a similar mass, we do not have unambiguous lattice operators to determine D_- and F_- but rather operators, which have an admixture of $D_\pm$ and $F_\pm$ respectively. We label these operators as $D_\pm$ and $F_\pm$ (cf. Table 2).

We have also replaced the light quark fields in the physical basis $\psi^{(u)}$ by their counterparts in the twisted basis $\chi^{(u)}$. Note that trial states created by such twisted basis operators are not eigenstates of parity. Nevertheless, as we have discussed in section 2.4, it is possible to assign unambiguously a parity label to the masses extracted from the time dependence of such twisted basis correlators.

3.1.3 Smearing techniques

When performing a lattice study of the static-light meson spectrum, the following points have to be considered:

- It is imperative to use trial states with large overlap to low lying energy eigenstates. Only then the corresponding meson masses can be extracted from correlation functions at small temporal separations, where signal-to-noise ratios are acceptable.
- To determine excited states for a given $\mathrm{O_h}$ representation, it is necessary to have a whole set of linearly independent trial states belonging to that $\mathrm{O_h}$ representation.

To fulfill both requirements we use different "radii" r (cf. eqns. (21) and (22)) and apply APE smearing and Gaussian smearing also with different parameters. The resulting extended trial states have significantly better overlap to low lying energy eigenstates than their unsmeared counterparts.

APE smearing of spatial links

After N_{APE} iterations APE smeared spatial links [25] are given by

$$U^{(N_{\mathrm{APE}})}(x, x+e_k) = P_{\mathrm{SU(3)}}\Bigg(U^{(N_{\mathrm{APE}}-1)}(x, x+e_k) + \alpha_{\mathrm{APE}} \sum_{j=\pm1,\pm2,\pm3}^{j\neq\pm k} U^{(N_{\mathrm{APE}}-1)}(x, x+e_j)$$
$$U^{(N_{\mathrm{APE}}-1)}(x+e_j, x+e_j+e_k) U^{(N_{\mathrm{APE}}-1)}(x+e_j+e_k, x+e_k)\Bigg), \quad (23)$$

where $U^{(0)}$ are the original unsmeared links. α_{APE} is a weight parameter and $P_{\mathrm{SU(3)}}$ denotes a projection back to SU(3) defined by

$$P_{\mathrm{SU(3)}}(U) = \frac{U'}{\det(U')^{1/3}} \quad , \quad U' = U\Big(U^\dagger U\Big)^{-1/2} \quad (24)$$

with $\det(U')^{1/3}$ being that root closest to 1.

Gaussian smearing of light quark operators

After N_{Gauss} iterations Gaussian smeared light quark operators [26, 27] are given by

$$\chi^{(N_{\mathrm{Gauss}})}(x) =$$
$$= \frac{1}{1+6\kappa}\Bigg(\chi^{(N_{\mathrm{Gauss}}-1)}(x) + \kappa_{\mathrm{Gauss}} \sum_{j=\pm1,\pm2,\pm3} U^{(N_{\mathrm{APE}})}(x, x+e_j)\chi^{(N_{\mathrm{Gauss}}-1)}(x+e_j)\Bigg), \quad (25)$$

where $\chi^{(0)}$ are the original unsmeared light quark operators and $U^{(N_{\mathrm{APE}})}$ denote APE smeared spatial links.

3.2 Correlation matrices

For each $\mathrm{O_h}$ representation we compute 6×6 correlation matrices

$$C_{KK'}(t) = \Big\langle \mathcal{O}^{(K)}(t)(\mathcal{O}^{(K')})^\dagger(0)\Big\rangle, \quad (26)$$

where $\mathcal{O}^{(K)}$ is a static-light meson creation operator (cf. eqns. (21) and (22)) with K denoting its parameters, i.e. $K = (\Gamma\,,\, N_{\mathrm{Gauss}}\,,\, r)$ (we have chosen $N_{\mathrm{APE}} = 10$, $\alpha_{\mathrm{APE}} = 0.5$ and $\kappa_{\mathrm{Gauss}} = 0.5$ for all operators). Detailed information about the operator content of the correlation matrices is given in Table 3.

The width of a Gaussian smeared light quark operator (25) in lattice units is approximately given by

$$\sigma \approx \sqrt{\frac{2N_{\mathrm{Gauss}}\kappa_{\mathrm{Gauss}}}{1+6\kappa_{\mathrm{Gauss}}}}. \quad (27)$$

O_h	Γ	N_{Gauss}	r	R/a	R in fm
A_1	γ_5	30	3	5.61	0.48
		60	6	9.00	0.77
	1	30	3	5.61	0.48
		60	6	9.00	0.77
	$\gamma_5\gamma_j x_j$	30	3	5.61	0.48
	$\gamma_j x_j$	30	3	5.61	0.48
E	$\gamma_1 x_1 - \gamma_2 x_2$ (and cyclic)	30	3	5.61	0.48
		60	6	9.00	0.77
		90	3	8.74	0.75
	$\gamma_5(\gamma_1 x_1 - \gamma_2 x_2)$ (and cyclic)	30	3	5.61	0.48
		60	6	9.00	0.77
		90	3	8.74	0.75
A_2	$\gamma_1 x_2 x_3 + \gamma_2 x_3 x_1 + \gamma_3 x_1 x_2$	30	2	5.88	0.50
		60	4	9.64	0.82
		90	2	8.91	0.76
	$\gamma_5(\gamma_1 x_2 x_3 + \gamma_2 x_3 x_1 + \gamma_3 x_1 x_2)$	30	2	5.88	0.50
		60	4	9.64	0.82
		90	2	8.91	0.76

Table 3: static-light meson creation operators used for the A_1, E and A_2 correlation matrices.

For $\kappa_{\mathrm{Gauss}} = 0.5$ and $N_{\mathrm{Gauss}} = (30\,,\,60\,,\,90)$ this amounts to $\sigma \approx (2.74\,,\,3.87\,,\,4.74)$. Taking also the parameter r into account one can estimate the radius of a static-light trial state: $R/a = \sqrt{r^2 + 3\sigma^2}$ for the A_1 and E representations and $R/a = \sqrt{3r^2 + 3\sigma^2}$ for the A_2 representation. The radii of the trial states used are also listed in Table 3 both in lattice units and in physical units.

Note that to identify the parity of states extracted via fitting it is important to compute correlation matrices, which contain for each operator Γ also its counterpart $\gamma_5\Gamma$ (cf. section 2.4).

3.2.1 Quark propagators

When evaluating the correlations (26), both static quark propagators and light quark propagators appear. To improve signal-to-noise ratios, we apply the following techniques.

Static quark propagators

To improve the signal to noise ratio for static-light correlation functions, we use the HYP2 static action [28, 29, 30]. Static quark propagators are given by

$$\Big\langle Q(x)\bar{Q}(y)\Big\rangle_{Q,\bar{Q}} \;=\; \delta^{(3)}(\mathbf{x}-\mathbf{y})U^{(\mathrm{HYP2})}(x;y)\bigg(\Theta(y_0-x_0)\frac{1-\gamma_0}{2}+\Theta(x_0-y_0)\frac{1+\gamma_0}{2}\bigg), \quad (28)$$

where $\langle\ldots\rangle_{Q,\bar{Q}}$ denotes the integration over the static quark fields and $U(x;y)$ is a path ordered product of HYP2 smeared links along the straight path from x to y.

Light quark propagators

To exploit translational invariance, it is imperative to use stochastic methods for the light quark propagators. The correlators can then be evaluated at a large number of source points, while only a few inversions of the lattice Dirac operator have to be performed. One very powerful method is maximal variance reduction [1]. A somewhat easier method to implement is to use stochastic sources on time slices and this has been found to give reasonable results [31]. Because we have inverted from such time-slice sources as part of our light-light meson studies [20, 21, 22], we follow this latter route, since it is computationally much quicker for us.

For each gauge configuration we use N_s stochastic $\mathcal{Z}_2\times\mathcal{Z}_2$ sources $\xi^{(\alpha)}$, $\alpha=1,\ldots,N_s$ located on the same timeslice. For our lightest three μ_q values we take $N_s=4$ sources, which are the same for each of the four spin components so that we can re-use previous inversions [20, 21, 22]. For our heavier two μ_q values, we had to redo the inversions so we use only $N_s=1$ source with random values in each of the spin components.

After solving

$$D^{(u)}_{\mathrm{Wtm}}(x;y)\phi^{(\alpha)}(y) \;=\; \xi^{(\alpha)}(x), \quad (29)$$

where $D^{(u)}_{\mathrm{Wtm}}=D_{\mathrm{W}}+i\mu_{\mathrm{q}}\gamma_5$ is the twisted mass Dirac operator acting on $\chi^{(u)}$, the light quark propagator is given by the unbiased estimate

$$\Big\langle \chi^{(u)}(x)\bar{\chi}^{(u)}(y)\Big\rangle_{\chi,\bar{\chi}} \;=\; (D^{(u)}_{\mathrm{Wtm}})^{-1}(x;y) \;\approx\; \sum_{\alpha=1}^{N_s}\phi^{(\alpha)}(x)(\xi^{(\alpha)})^{\dagger}(y), \quad (30)$$

where $\langle\ldots\rangle_{\chi,\bar{\chi}}$ denotes the integration over the light quark fields.

3.3 Extracting static-light meson masses from correlation matrices

Assuming that for sufficiently large t the correlation matrix (26) can be approximated by the n lowest lying energy eigenstates $|i\rangle$, $i=1,\ldots,n$ we use the ansatz

$$\Big(\mathcal{O}^{(K)}\Big)^{\dagger}|\Omega\rangle \;\approx\; \sum_{i=1}^{n} b_i^K|i\rangle. \quad (31)$$

The correlation matrix (26) in terms of the ansatz is

$$C_{KK'}(t) \approx \sum_{i=1}^{n} (b_i^K)^* b_i^{K'} e^{-E_i t} = \tilde{C}_{KK'}(t). \tag{32}$$

The parameters E_i and b_i^K are determined by minimising

$$\chi^2 = \sum_{t=t_{\min}}^{t_{\max}} \sum_{K \leq K'} \left(\frac{C_{KK'}(t) - \tilde{C}_{KK'}(t)}{\sigma(C_{KK'}(t))} \right)^2, \tag{33}$$

where $\sigma(C_{KK'}(t))$ denotes the statistical error of $C_{KK'}(t)$.

In the following we apply this fitting procedure with $n = 4$ exponentials. To obtain physically meaningful results with small statistical errors, it is essential to determine an appropriate fitting range $t_{\min} \ldots t_{\max}$. To this end, we have performed correlated fits with various fitting ranges using eigenvalue smoothed covariance matrices [32]. We have found that $t_{\min} = 3$ gives reasonable reduced χ^2 values (cf. Table 4), while data points beyond $t_{\max} = 12$ seem to be dominated by statistical noise, i.e. including them in the fits does not alter resulting meson masses nor corresponding statistical errors.

O_h	$\mu_q = 0.0040$	$\mu_q = 0.0064$	$\mu_q = 0.0085$	$\mu_q = 0.0100$	$\mu_q = 0.0150$
A_1	1.89	2.30	2.35	0.95	1.16
E	1.21	1.33	1.70	2.04	2.09
A_2	1.56	1.96	1.28	1.16	1.26

Table 4: χ^2/dof from correlated χ^2 fits for different O_h representations and different μ_q.

As has already been discussed in section 3.1.2, it is difficult to unambiguously determine the total angular momentum j of a state obtained from a lattice computation. This is, because for every O_h representation there exists an infinite number of possible total angular momentum eigenstates (cf. Table 2). In the following, we assume that the low lying states we are going to study have the lowest total angular momentum possible, i.e. we assign $j = 1/2$ to states from A_1, $j = 3/2$ to states from E and $j = 5/2$ to states from A_2. Parity on the other hand can directly be read off from the coefficients b_i^K (cf. section 2.4).

Since static-light meson masses diverge in the continuum limit due to the self energy of the static quark, we always consider mass differences, where this self energy cancels. Mass differences between various static-light mesons with quantum numbers $j^{\mathcal{P}}$ and the lightest static-light meson ($(1/2)^- \equiv S$ ground state) for all five μ_q values are collected in Figure 1 and Table 5. Statistical errors have been computed from 100 bootstrap samples.

To check the stability of the fitting method, we have performed computations with different parameters (number of states n, fitting range $t_{\min} \ldots t_{\max}$, operator content of the correlation matrices). We have obtained results which are consistent within statistical errors.

$j^{\mathcal{P}}$	$\mu_q = 0.0040$	$\mu_q = 0.0064$	$\mu_q = 0.0085$	$\mu_q = 0.0100$	$\mu_q = 0.0150$
$(1/2)^{-,*} \equiv S^*$	777(17)	808(19)	839(22)	780(34)	782(32)
$(1/2)^{+} \equiv P_-$	389(16)	428(12)	447(10)	456(17)	495(16)
$(3/2)^{+} \equiv P_+$	473(10)	496(8)	488(7)	486(12)	479(14)
$(3/2)^{-} \equiv D_\pm$	813(24)	828(19)	833(16)	861(27)	858(21)
$(5/2)^{-} \equiv D_+$	823(24)	887(14)	887(15)	862(24)	846(42)
$(5/2)^{+} \equiv F_\pm$	1134(35)	1205(27)	1173(24)	1136(34)	1205(28)

Table 5: static-light mass differences $m(j^{\mathcal{P}}) - m(S)$ in MeV for different μ_q.

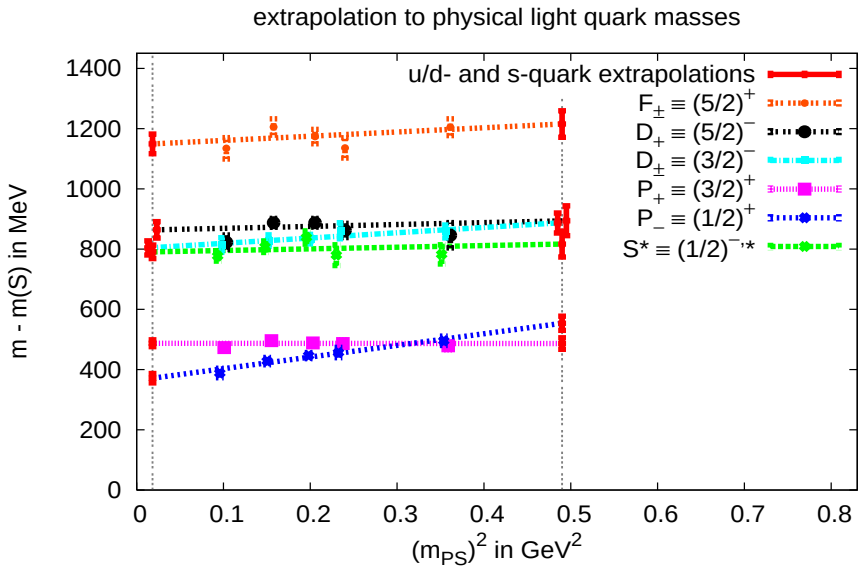

Figure 1: static-light mass differences linearly extrapolated to the physical u/d quark mass and the physical s quark mass.

3.4 Extrapolation to physical light quark masses

We linearly extrapolate our static-light mass differences in $(m_{\rm PS})^2$ to the physical u/d quark mass ($m_{\rm PS} = 135\,\text{MeV}$) and the physical s quark mass (taken here as $m_{\rm PS} = 700\,\text{MeV}$). Results are shown in Figure 1 and Table 6. We also list the corresponding χ^2/dof values indicating that straight lines are acceptable for extrapolation. A more thorough study using extrapolations based on chiral effective theories will be attempted when we are able to extract the continuum limit of our results at each light quark mass value.

Note that we consider the unitary sector, where valence quarks and sea quarks are of the same mass. For the s quark extrapolated results this implies a sea of two degenerate s instead of a sea of u and d. If the sea-quark mass dependence of our spectra is small, as usually assumed, then our results will be a good estimate of the physical static-strange meson spectrum. This

$j^{\mathcal{P}}$	u/d quark extrapolation: $m(j^{\mathcal{P}}) - m(S)$ in MeV	s quark extrapolation: $m(j^{\mathcal{P}}) - m(S)$ in MeV	χ^2/dof
$(1/2)^{-,*} \equiv S^*$	791(23)	816(43)	1.82
$(1/2)^+ \equiv P_-$	371(16)	554(23)	0.44
$(3/2)^+ \equiv P_+$	487(11)	486(19)	1.22
$(3/2)^- \equiv D_\pm$	804(23)	887(33)	0.21
$(5/2)^- \equiv D_+$	864(27)	894(50)	2.24
$(5/2)^+ \equiv F_\pm$	1149(33)	1215(44)	1.40

Table 6: static-light mass differences linearly extrapolated to the physical u/d quark mass and the physical s quark mass.

limitation can be removed, in principle, by performing similar computations on $N_f = 2+1+1$ flavour gauge configurations, which are currently being produced by ETMC [33].

We have performed a similar extrapolation for the mass difference of the P wave states. When extrapolating to the physical u/d quark mass, we find $m(P_+) - m(P_-) = 117(17)\,\text{MeV}$, i.e. the $P_- \equiv (1/2)^+$ state is lighter than the $P_+ \equiv (3/2)^+$ as usually expected. When increasing the mass of the light quark, we observe a reversal of this level ordering, $m(P_-) - m(P_+) = 71(23)\,\text{MeV}$ at the physical s quark mass. It will be interesting to study this in the continuum limit, in particular since such a reversal is predicted by certain phenomenological models [12, 13, 14, 15].

In principle, our excited states could be two-particle states since we have dynamical sea quarks. In practice, the two-particle state is expected to be weakly coupled to the operators we use (which are constructed assuming one particle states). Some exploration of transitions to two particle static-light mesons has been made which confirms this expectation [31].

4 Predictions for B and B_s mesons

To make predictions regarding the spectrum of B and B_s mesons, we interpolate between the static-light lattice results obtained in the previous section and experimental results for charmed mesons[2] [11]. To this end, we assume a linear dependence in $1/m_Q$, where m_Q is the mass of the heavy quark. This interpolation introduces a possible systematic error, which, however, we consider to be smaller than the systematic errors coming from the continuum limit, the extrapolation to light quarks and the treatment of the strange sea. The most important of these systematic errors is that involved in the continuum limit and that will be quantified when we have results at finer lattice spacings.

[2]For the states B, D, D^*, D_0^* and D_2^* experimental results for charged as well as for uncharged mesons exist. We use the average in the following.

4.1 B mesons

Results of the interpolation between our u/d extrapolated P wave lattice results and experimental results on D mesons are shown in Figure 2a and Table 7.

- To predict $m(B_0^*) - m(B)$ and $m(B_1^*) - m(B)$, we interpolate between our static spin degenerate $P_- \equiv (1/2)^+$ state, i.e. $m(P_-) - m(S)$, and experimental data on $m(D_0^*) - m(D)$ and $m(D_1(2430)^0) - m(D)$.
- To predict $m(B_1) - m(B)$ and $m(B_2^*) - m(B)$, we interpolate between our static spin degenerate $P_+ \equiv (3/2)^+$ state, i.e. $m(P_+) - m(S)$, and experimental data on $m(D_1(2420)^0) - m(D)$ and $m(D_2^*) - m(D)$. Here we assign the D_1^0 states assuming that states with similar widths belong to the same multiplet.
- The line labeled "$S \equiv (1/2)^-$" in Figure 2a shows that $m(B^*) - m(B)$ is lighter by a factor of $\approx m_c/m_b$ than $m(D^*) - m(D)$ indicating that a straight line is a suitable ansatz for interpolation and that the estimate of $m_c/m_b = 0.3$ [11] is reasonable.
- A comparison with experimental results from CDF and DØ [34, 35] on $m(B_1) - m(B)$ and $m(B_2^*) - m(B)$ shows that our lattice results are larger by $\approx 10\%$ (cf. Table 7). There is another resonance listed in [11] with unknown quantum numbers $J^{\mathcal{P}}$, $m(B_J^*) - m(B)$, which is rather close to our $m(B_0^*) - m(B)$ and $m(B_1^*) - m(B)$ results. For a conclusive comparison it will be necessary to study the continuum limit, which will be part of an upcoming publication.

	$m - m(B)$ in MeV					$m - m(B_s)$ in MeV			
state	lattice	CDF	DØ	PDG	state	lattice	CDF	DØ	PDG
B_0^*	413(19)				B_{s0}^*	493(16)			
B_1^*	428(19)				B_{s1}^*	535(16)			
B_1	508(8)	454(5)	441(4)		B_{s1}	510(13)	463(1)		
B_2^*	519(8)	458(6)	467(4)		B_{s2}^*	521(13)	473(1)	473(2)	
B_J^*				418(8)	B_{sJ}^*				487(16)

Table 7: lattice and experimental results for P wave B and B_s states. Errors on lattice results are statistical only.

4.2 B_s mesons

For B_s mesons we proceed in the same way as for B mesons, using our s quark extrapolated static-light lattice results and experimental results on D_s mesons (cf. Figure 2b and Table 7).

- To predict $m(B_{s0}^*) - m(B_s)$ and $m(B_{s1}^*) - m(B_s)$, we interpolate between our static spin degenerate $P_- \equiv (1/2)^+$ state, i.e. $m(P_-) - m(S)$, and experimental data on $m(D_{s0}^*) - m(D_s)$ and $m(D_{s1}(2460)) - m(D_s)$.

a) Excited B meson masses

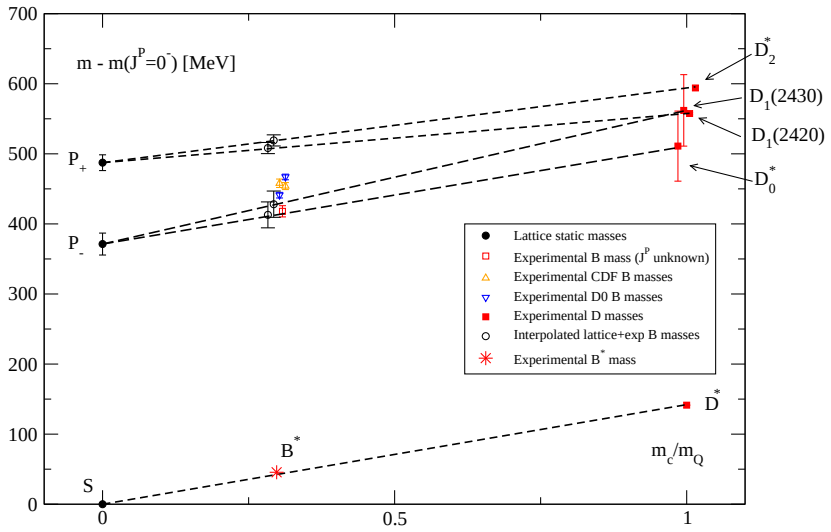

b) Excited B_s meson masses

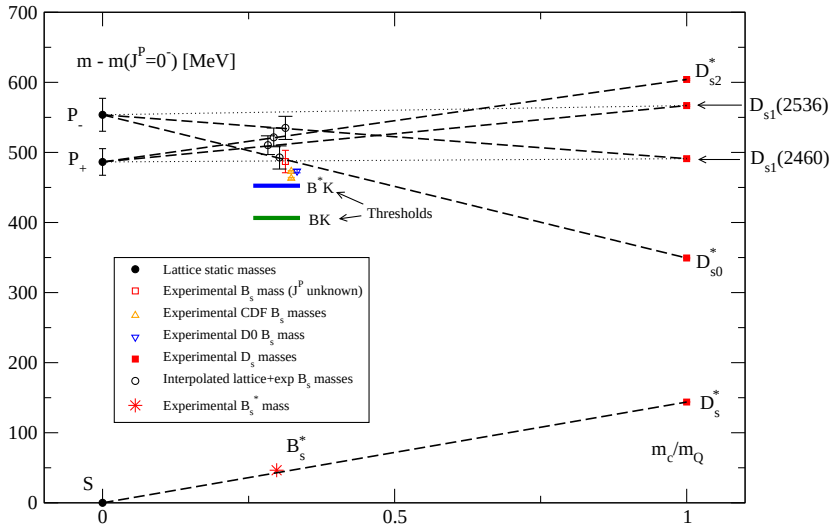

Figure 2: Static-light mass differences linearly interpolated to the physical b quark mass.

- To predict $m(B_{s1}) - m(B_s)$ and $m(B^*_{s2}) - m(B_s)$, we interpolate between our static spin degenerate $P_+ \equiv (3/2)^+$ state, i.e. $m(P_+) - m(S)$, and experimental data on $m(D_{s1}(2536)) - m(D_s)$ and $m(D_{s2}) - m(D_s)$. This time we assign the D_{s1} states according to the expectation that the splitting between $D_{s1}(\text{“}j = 3/2\text{”})$ and D_{s2} is roughly

$m_b/m_c \approx 3.3$ times larger than that between B_{s1} and B^*_{s2}, which is according to [36] approximately 10 MeV. We also illustrate the opposite assignment in Figure 2b for completeness.

- The line labeled "$S \equiv (1/2)^-$" in Figure 2b shows that $m(B^*_s) - m(B_s)$ is lighter by a factor of $\approx m_c/m_b$ than $m(D^*_s) - m(D_s)$ indicating that a straight line is a suitable ansatz for interpolation and that the estimate of $m_c/m_b = 0.3$ [11] is reasonable.

- A comparison with experimental results from CDF and DØ [36, 37] on $m(B_1) - m(B^0)$ and $m(B^*_2) - m(B^0)$ shows that our lattice results are larger by $\approx 10\%$ (cf. Table 7). There is another resonance listed in [11] with unknown quantum numbers $J^{\mathcal{P}}$, $m(B^*_{sJ}) - m(B_s)$, which is rather close to our $m(B^*_{s0}) - m(B_s)$ result. For a conclusive comparison it will be necessary to study the continuum limit, which will be part of an upcoming publication.

- We also plot the BK and B^*K thresholds in Figure 2b. The fact that our lattice results on the P wave states B^*_{s0}, B^*_{s1}, B_{s1} and B^*_{s2} are larger indicates that corresponding decays are energetically allowed. Therefore, one should expect that these states may have a larger width compared to the corresponding excited D_s states.

5 Conclusions

We have explored the low lying static-light meson spectrum using $N_f = 2$ flavours of sea quarks with Wtm lattice QCD. We have presented results for total angular momentum of the light degrees of freedom $j = 1/2$, $j = 3/2$ and $j = 5/2$ and for parity $\mathcal{P} = +$ and $\mathcal{P} = -$. The lattice spacing is $a = 0.0855(5)$ fm and we have considered five different values for the light quark mass corresponding to $300\,\text{MeV} \lesssim m_{\text{PS}} \lesssim 600\,\text{MeV}$.

We have extrapolated our results in $(m_{\text{PS}})^2$ both to the physical u/d quark mass and to the physical s quark mass. Moreover, we used experimental results from D and D_s mesons to interpolate in the heavy quark mass from the static case to the physical b quark mass. We are able to predict the spectrum of excited B and B_s mesons from first principles. Our formalism has lattice artifacts of order a^2 and we shall be able to control these in future work by studying smaller a values. Comparing our current predictions to available experimental results, we find agreement up to 10% with P wave B and B_s mesons.

Throughout this paper we have considered the unitary sector, where valence quarks and sea quarks are of the same mass. Particularly for our B_s results, this implies a sea of two degenerate s instead of a sea of u and d. We plan to improve this by performing similar computations on $N_f = 2 + 1 + 1$ flavour gauge configurations, which are currently produced by ETMC. Another important issue in the near future will be an investigation of the continuum limit, which amounts to considering other values for the lattice spacing. Such a study will be necessary for a conclusive comparison between lattice results and experimental results for B and B_s mesons. We also plan to compute static-light decay constants and to make a detailed comparison with chiral effective Lagrangians.

Acknowledgments

MW would like to thank Carsten Urbach for help in retrieving and handling ETMC gauge configurations. Moreover, we acknowledge useful discussions with Benoit Blossier, Tommy Burch, Vladimir Galkin, Christian Hagen, Rainer Sommer and Carsten Urbach. This work has been supported in part by the DFG Sonderforschungsbereich/Transregio SFB/TR9-03.

References

[1] C. Michael and J. Peisa [UKQCD Collaboration], "Maximal variance reduction for stochastic propagators with applications to the static quark spectrum," Phys. Rev. D **58**, 034506 (1998) [arXiv:hep-lat/9802015].

[2] A. M. Green, J. Koponen, C. McNeile, C. Michael and G. Thompson [UKQCD Collaboration], "Excited B mesons from the lattice," Phys. Rev. D **69**, 094505 (2004) [arXiv:hep-lat/0312007].

[3] T. Burch and C. Hagen, "Domain decomposition improvement of quark propagator estimation," Comput. Phys. Commun. **176**, 137 (2007) [arXiv:hep-lat/0607029].

[4] J. Koponen, "Energies and radial distributions of B_s mesons on the lattice," Acta Phys. Polon. B **38**, 2893 (2007) [arXiv:hep-lat/0702006].

[5] J. Foley, A. O'Cais, M. Peardon and S. M. Ryan, "Radial and orbital excitations of static-light mesons," Phys. Rev. D **75**, 094503 (2007) [arXiv:hep-lat/0702010].

[6] J. Koponen [UKQCD Collaboration], "Energies of B_s meson excited states - a lattice study," arXiv:0708.2807 [hep-lat].

[7] T. Burch, C. Hagen, C. B. Lang, M. Limmer and A. Schafer, "Excitations of singly beautiful hadrons," arXiv:0809.1103 [hep-lat].

[8] K. Jansen, C. Michael, A. Shindler and M. Wagner [ETM Collaboration], "Static-light meson masses from twisted mass lattice QCD," arXiv:0808.2121 [hep-lat].

[9] M. Bochicchio, G. Martinelli, C.R. Allton, C.T Sachrajda and D.B. Carpenter, "Heavy quark spectroscopy on the lattice" Nucl. Phys. B **B372**, 403, (1992).

[10] D. Guazzini, H.B. Meyer and R. Sommer [ALPHA Collaboration] "Non-perturbative renormalisation of the chromo-magnetic operator in heavy quark effective theory and the $B^* - B$ mass splitting" JHEP **0710**, 081 (2007) [arXiv:0705.1809 [hep-lat]].

[11] W.-M. Yao *et al.* [Particle Data Group], J. Phys. G **33**, 1 (2006) and 2007 partial update for the 2008 edition.

[12] H. J. Schnitzer, "Spin structure in meson spectroscopy with an effective scalar confinement of quarks," Phys. Rev. D **18**, 3482 (1978).

[13] H. J. Schnitzer, "Where are the inverted multiplets of meson spectroscopy?," Phys. Lett. B **226** (1989) 171.

[14] D. Ebert, V. O. Galkin and R. N. Faustov, "Mass spectrum of orbitally and radially excited heavy-light mesons in the relativistic quark model," Phys. Rev. D **57**, 5663 (1998) [Erratum-ibid. D **59**, 019902 (1999)] [arXiv:hep-ph/9712318].

[15] N. Isgur, "Spin-orbit inversion of excited heavy quark mesons," Phys. Rev. D **57**, 4041 (1998).

[16] P. Weisz, "Continuum Limit Improved Lattice Action For Pure Yang-Mills Theory. 1," Nucl. Phys. B **212**, 1 (1983).

[17] R. Frezzotti, P. A. Grassi, S. Sint and P. Weisz [Alpha collaboration], "Lattice QCD with a chirally twisted mass term," JHEP **0108**, 058 (2001) [arXiv:hep-lat/0101001].

[18] R. Frezzotti and G. C. Rossi, "Chirally improving Wilson fermions. I: O(a) improvement," JHEP **0408**, 007 (2004) [arXiv:hep-lat/0306014].

[19] A. Shindler, "Twisted mass lattice QCD," Phys. Rept. **461**, 37 (2008) [arXiv:0707.4093 [hep-lat]].

[20] Ph. Boucaud *et al.* [ETM Collaboration], "Dynamical twisted mass fermions with light quarks," Phys. Lett. B **650**, 304 (2007) [arXiv:hep-lat/0701012].

[21] C. Urbach [ETM Collaboration], "Lattice QCD with two light Wilson quarks and maximally twisted mass," PoS **LAT2007**, 022 (2007) [arXiv:0710.1517 [hep-lat]].

[22] Ph. Boucaud *et al.* [ETM Collaboration], "Dynamical twisted mass fermions with light quarks: simulation and analysis details," arXiv:0803.0224 [hep-lat].

[23] M. Kurth and R. Sommer [ALPHA Collaboration], "Renormalization and $\mathcal{O}(a)$ improvement of the static axial current," Nucl. Phys. B **597**, 488 (2001) [arXiv:hep-lat/0007002].

[24] P. Lacock, C. Michael, P. Boyle and P. Rowland [UKQCD Collaboration], "Orbitally excited and hybrid mesons from the lattice," Phys. Rev. D **54** 6997 (1996) [arXiv:hep-lat/9605025].

[25] M. Albanese *et al.* [APE Collaboration], "Glueball masses and string tension in lattice QCD," Phys. Lett. B **192**, 163 (1987).

[26] S. Gusken, "A study of smearing techniques for hadron correlation functions," Nucl. Phys. Proc. Suppl. **17** (1990) 361.

[27] C. Alexandrou *et al.* [ETM Collaboration], "Light baryon masses with dynamical twisted mass fermions," Phys. Rev. D **78**, 014509 (2008) [arXiv:0803.3190 [hep-lat]].

[28] A. Hasenfratz and F. Knechtli, "flavour symmetry and the static potential with hypercubic blocking," Phys. Rev. D **64**, 034504 (2001) [arXiv:hep-lat/0103029].

[29] M. Della Morte *et al.*, "Lattice HQET with exponentially improved statistical precision," Phys. Lett. **B581**, 93, (2004) [arXiv:hep-lat/0307021].

[30] M. Della Morte, A. Shindler and R. Sommer, "On lattice actions for static quarks," JHEP **0508**, 051 (2005) [arXiv:hep-lat/0506008].

[31] C. McNeile, C. Michael and G. Thompson [UKQCD Collaboration], "Hadronic decay of a scalar B meson from the lattice," Phys. Rev. D **70**, 054501 (2004) [arXiv:hep-lat/0404010].

[32] C. Michael and A. McKerrell, "Fitting correlated hadron mass spectrum data," Phys. Rev. D **51**, 3745 (1995) [arXiv:hep-lat/9412087].

[33] T. Chiarappa *et al.*, "Numerical simulation of QCD with u, d, s and c quarks in the twisted-mass Wilson formulation," Eur. Phys. J. C **50**,373 (2007) [arXiv:hep-lat/0606011].

[34] R. K. Mommsen, "B_c and excited B states: a Tevatron review," Nucl. Phys. Proc. Suppl. **170**, 172 (2007) [arXiv:hep-ex/0612003].

[35] V. M. Abazov *et al.* [D0 Collaboration], "Observation and properties of $L = 1$ B_1 and B_2^* mesons," Phys. Rev. Lett. **99**, 172001 (2007) [arXiv:0705.3229 [hep-ex]].

[36] T. Aaltonen *et al.* [CDF Collaboration], "Observation of orbitally excited B_s mesons," Phys. Rev. Lett. **100**, 082001 (2008) [arXiv:0710.4199 [hep-ex]].

[37] V. M. Abazov *et al.* [D0 Collaboration], "Observation and properties of the orbitally excited B_{s2}^* meson," Phys. Rev. Lett. **100**, 082002 (2008) [arXiv:0711.0319 [hep-ex]].